Transplantation of Engineered Chimeric Liver With Autologous Hepatocytes and Xenobiotic Scaffold

Toshiyuki Hata, MD,† Shinji Uemoto, MD, PhD,* Yasuhiro Fujimoto, MD, PhD,* Takashi Murakami, MD, PhD,‡ Chise Tateno, PhD,§ Katsutoshi Yoshizato, PhD,§ and Eiji Kobayashi, MD, PhD||*

Objective: Generation of human livers in pigs might improve the serious shortage of grafts for human liver transplantation, and enable liver transplantation without the need for deceased or living donors. We developed a chimeric liver (CL) by repopulation of rat hepatocytes in a mouse and successfully transplanted it into a rat recipient with vessel reconstruction. This study was designed to investigate the feasibility of CL for supporting the recipient after auxiliary liver grafting.

Methods: Hepatocytes from luciferase transgenic or luciferase/LacZ double-transgenic rats were transplanted into 20- to 30-day-old urokinase-type plasminogen activator/severe-combined immunodeficiency (uPA/SCID) mice (n = 40) to create CLs with rat-origin hepatocytes. After replacement of mouse hepatocytes with those from rats, the CLs were transplanted into wild-type Lewis (n = 30) and analbuminemia (n = 10) rats, followed by immunosuppression using tacrolimus (TAC) with/without cyclophosphamide (CPA) or no immunosuppression. Organ viability was traced by in vivo bioimaging and Doppler ultrasonography in the recipient rats for 4 to 6 months. Rat albumin production was also evaluated in the analbuminemia rats for 4 months. In addition, histological analyses including Ki67 proliferation staining were performed in some recipients.

Results: Both immunosuppressive protocols significantly improved graft survival and histological rejection of CLs as compared to the nonimmunosuppressed group. Although rat albumin production was maintained in the recipients for 4 months after transplantation, ultrasonography revealed patent circulation in the grafts for 6 months. Ki67 staining analysis also revealed the regenerative potential of CLs after a hepatectomy of the host native liver, whereas immune reactions still remained in the mouse-origin structures.

Conclusions: This is the first report showing that engineered CLs have potential as alternative grafts to replace the use of grafts from human donors.

Keywords: alternative organ graft, auxiliary liver transplantation, chimeric liver, engineered organ, liver transplantation

(*Ann Surg* 2013;257: 542–547)

From the *Division of Hepato-Biliary-Pancreatic and Transplant Surgery, Department of Surgery, Graduate School of Medicine, Kyoto University, Kyoto, Japan; †Division of Transplantation Surgery, Mayo Clinic Florida, Jacksonville; ‡Department of Pharmacy, Takasaki University of Health and Welfare, Gunma, Japan; §PhoenixBio Co Ltd, Higashi-Hiroshima, Japan; and ||Division of Development of Advanced Treatment, Center for Development of Advanced Medical Technology, Jichi Medical University, Tochigi, Japan.

Disclosure: Supported by a Grant-in-Aid for Scientific Research (No 20249058) from the Japan Society for the Promotion of Science, the "Strategic Research Platform" for Private Universities, a matching fund subsidy from the Ministry of Education, Culture, Sports, Science and Technology of Japan (2008), the COE program from MEXT (2008), and the Kyoto University Foundation (2011). E.K. is a chief scientific advisor for Otsuka Pharmaceutical Factory, Inc. This work was not supported by any funding from the National Institute of Health, Wellcome Trust, or Howard Hughes Medical Institute.

Supplemental digital content is available for this article. Direct URL citations appear in the printed text and are provided in the HTML and PDF versions of this article on the journal's Web site (www.annalsofsurgery.com).

Reprints: Eiji Kobayashi, MD, PhD, 3311-1 Yakushiji, Shimotsuke, Tochigi 329-0498, Japan.E-mail: eijikoba@jichi.ac.jp.

ISSN: 0003-4932/13/25703-0542
DOI: 10.1097/SLA.0b013e31825c5349

Liver transplantation is currently regarded as the most effective treatment for end-stage liver diseases. Because the worldwide graft shortage remains unresolved,[1,2] engineered organs are anticipated as alternative grafts to fill the scarcity and ultimately replace those from deceased and living donors. Although regenerative technology has already developed various kinds of regenerative cells and tissues,[3,4] they are still insufficient to cure patients with end-stage liver diseases because of the absence of complicated functions and limited volume. Therefore, a regenerative liver graft for use as an "organ" is required. To achieve an appropriate 3-dimensional structure and differentiation to specific tissues in a single organ, application of native organs as scaffolds has been reported as a possible solution.[5–7] Recent advances in genetic manipulation of animals such as pigs have produced transgenic animals with a lower risk of xenorejection.[8,9] Thus, using their native organogenetic potentials, development of engineered liver "organs" is expected.[10] In such a protocol, human hepatocytes are transplanted to a transgenic pig to replace its native hepatocytes, resulting in development of a chimeric liver (CL) with human parenchyma and swine nonparenchymal components, including vessels, bile ducts, and other connecting tissues. However, it is unclear whether such engineered CLs can be transplanted into recipients, or whether they can maintain their organ structures and functions after transplantation. In this study, we developed a rodent model of chimeric liver transplantation to investigate its feasibility (Fig. 1A). We used mice and rats as substitutes for transgenic pigs and humans, respectively, and created CLs in transgenic mice using hepatocytes derived from transgenic rats. After chimeric liver transplantation into rat recipients with vessel reconstruction, we examined the long-term viability and functions of the transplanted CL grafts.

MATERIALS AND METHODS

Animals

All mice and rats were housed in a temperature-controlled environment under a 12-hour light-dark cycle with free access to water and standard rodent chow diet. Male and female albumin enhancer-/promoter-driven urokinase-type plasminogen activator/severe-combined immunodeficiency (uPA/SCID) mice (Phoenixbio Co, Ltd, Japan) (n = 40), which express and accumulate urokinase-type plasminogen specifically in native hepatocytes, resulting in liver disease,[11,12] were used as the scaffolds for CL regeneration. Male luciferase transgenic Lewis (Luc-LEW) (MHC haplotype; $RT1^l$)[13] (n = 2), and female luciferase and LacZ double-transgenic Lewis (Luc/LacZ-LEW) ($RT1^l$) rats[14] (n = 1) were used as hepatocyte donors. Male wild-LEW rats ($RT1^l$) (Charles River Japan, Japan) (n = 30) and male Nagase analbuminemia rats ($RT1^a$)[15] (Japan SLC, Japan) (n = 10) were used as the recipients of chimeric liver transplantation. All experiments in this study were performed in accordance with the Jichi Medical University Guide for Laboratory Animals after approval by the ethics committee of PhoenixBio Co, Ltd.

Generation of CLs

Isolated hepatocytes were obtained from 10-week-old Luc-LEW and Luc/LacZ LEW rats using a standard 2-step collagenase

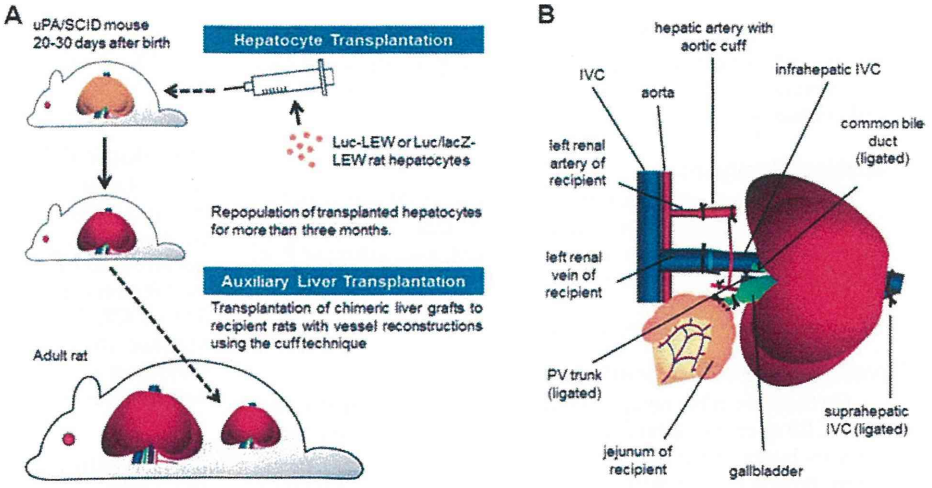

FIGURE 1. A, Experimental protocol used for Chimeric liver transplantation. B, Schema of engraftment of CL into recipient rat.

perfusion method.[16] Collagenase (75 mg/body) (COLLAGENASE S-1; Nitta-gelatin, Japan) was perfused through the portal vein, then 5.0 $\times$ 10^5 hepatocytes were transplanted into 20- to 30-day-old uPA/SCID mice, as previously reported.[12] These mice were kept for 3 months to obtain CLs with satisfactory size (mean $\pm$ SEM, 1.69 $\pm$ 0.04 g) and chimerism.

Harvesting of CLs

The CLs were harvested from uPA/SCID mice along with the hepatic artery with the aortic cuff and infrahepatic inferior vena cava. The portal vein trunk, common bile duct, and suprahepatic inferior vena cava were ligated. After systemic injection of 300 U of heparin sodium (Novo-Heparin; Mochida, Japan), the graft was harvested and cryo-preserved in 0.9% saline. A 10-mm plastic tube (22G SurfloR, IV catheter; Terumo, Japan) was inserted into the gallbladder, and a plastic cuff (18G SurfloR) was installed onto the end of the infrahepatic inferior vena cava.

Auxiliary Liver Transplantation of CLs

The CLs were engrafted in an auxiliary manner with vessel reconstruction using a cuff technique, as we previously reported.[17] In brief, after a simple left nephrectomy, a plastic cuff (22G SurfloR) was installed on the end of the recipient left renal artery. The graft hepatic artery and infrahepatic inferior vena cava were anastomosed to the recipient left renal artery and vein, respectively (see Video and Figure, Supplemental Digital Contents 1 and 2, demonstrating reperfusion of graft, available at http://links.lww.com/SLA/A254 and http://links.lww.com/SLA/A256, respectively). The graft gallbladder was connected to the recipient jejunum (Fig. 1B) and the recipient liver was left intact. There were no significant differences regarding any of the parameters for the animals and surgical procedures (data not shown). Recipient rats that died within 24 hours after chimeric liver transplantation or showed no luminescent signals on day 1 were excluded from postoperative analyses.

PostTransplant Treatment

Solid immunosuppressive protocols with tacrolimus (TAC) for T cell-mediated rejection and cyclophosphamide (CPA) for antibody-mediated rejection were used. The LEW rat recipients were treated with one of the following protocols: daily tacrolimus [TAC (+)CPA (−)] (n = 15), daily tacrolimus and cyclophosphamide pretreatment [TAC (+)CPA(+)] (n = 6), or no immunosuppression [TAC(−)CPA(−)] (n = 6). In the TAC(+)CPA(−) and TAC(+)CPA(+) groups, tacrolimus (Prograf; Astellas, Japan) was injected intramuscularly into the recipient rats at a dose of 0.64 mg/kg before and every day after transplantation. In TAC (+)CPA(+), candidate recipient rats were prepared with an intraperitoneal injection of cyclophosphamide (Endoxan, Shionogi, Japan) at a dose of 60 mg/kg 10 days before transplantation (dose of cyclophosphamide modified from previous report[18]). For Nagase analbuminemia rat recipients (n = 8), tacrolimus was given every day intramuscularly at a dose of 0.32 mg/kg. The recipient rats were observed daily and those in very poor condition were euthanized.

Evaluation of Luminescence From CLs

In vivo luciferase imaging of CLs was performed in both uPA/SCID mice for 3 months after hepatocyte transplantation and recipient rats throughout their survival after chimeric liver transplantation using a noninvasive bioimaging system (IVIS, Xenogen, CA), and the images were analyzed using a software package (Igor; WaveMetrics, OR, and IVIS Living Image; Xenogen). Before imaging, D-luciferin (potassium salt; Biosynth, Switzerland) (30 mg/kg) was injected into the peritoneal cavity of uPA/SCID mice or the penile vein of recipient rats. Signal intensity was quantified as photon flux in units of photons (s/cm^2/steradian) in the region of interest.

ELISA for Serum Rat Albumin Levels

Blood samples were obtained from uPA/SCID mice for 3 months after hepatocyte transplantation and Nagase analbuminemia rat recipients for 4 months after chimeric liver transplantation. To examine hepatic functions specific to CLs in our model with an intact recipient liver, we measured serum rat albumin using a Rat Albumin ELISA KIT (AKRAL-120, Shibayagi, Japan).

Histological Analyses

Tissue samples were fixed in 10% formalin for hematoxylin-eosin staining, and 10-μm thick sections were used. For X-gal and immunohistochemical staining, 4%-paraformaldehyde-fixed frozen samples were sliced into 4-μm thick sections. X-gal analyses were performed as previously reported.[14] Immunohistochemical analyses of the CL grafts were performed before and 2 days after the host left lobectomy with anti-Ki67 rabbit polyclonal antibody (RB-1510-P, Thermo Fisher Scientific, CA). Fifteen random views of each sample were obtained and Ki67-positive hepatocytes were separately counted in areas (mm^2) with viable hepatocytes using image software (Scion Image; Scion, MD).

Ultrasonographic Analyses

Blood flow velocities were measured using an ultrasound system (Prosound SSD-α5; ALOKA, Japan). Velocity was quantified in unit of cm/second.

Statistical Analyses

We performed statistical analyses using StatView5.0 (SAS, NC). We used the analysis of variance test and Holm-Sidak as a post hoc test. Data are presented as the mean ± SEM, with values of $P < 0.05$ considered to be statistically significant.

RESULTS

Development of CL Grafts in Mice

On the basis of the repopulation of transplanted rat hepatocytes in uPA/SCID mice, the spreading of positive areas was observed using in vivo bioluminescent imaging (Fig. 2A). Luminescent fluxes increased rapidly and reached a plateau for approximately 3 months after hepatocyte transplantation (Fig. 2B). Moreover, serum rat albumin concentration on day 30 was significantly higher than that on day 5, then remained until day 85 (Fig. 2C). Luminescent fluxes and albumin concentrations were strongly correlated (Spearman correlation coefficient $r = 0.86$, $P < 0.0001$), suggesting that luminescence reflected CL function. The appearance was that of a normal mouse liver (Fig. 2D). Although hematoxylin-eosin staining showed normal histological structures, X-gal staining revealed that the mouse hepatic parenchyma was nearly entirely replaced by LacZ-positive rat hepatocytes, except for the other hepatic components, such as the vessels and bile ducts in Glisson capsules (Fig. 2E).

Graft Viability After Auxiliary Transplantation

In the TAC(−)CPA(−) group, luminescence vanished rapidly until day 5 after Chimeric liver transplantation, whereas it was stably maintained for 4 weeks in both TAC(+)CPA(−) and TAC(+)CPA(+). There was no significant difference between those 2 groups (Fig. 3A).

Histological Analyses of Transplanted CL Grafts

Hematoxylin-eosin staining showed massive necrosis and destruction of the arrangement of the hepatic lobules in TAC(−)CPA(−) on day 5 (Fig. 3B). In contrast, TAC(+)CPA(−) on day 7 showed maintenance of those, even with massive cellular infiltration from the Glisson capsules to the central areas (Fig. 3C). Furthermore, in TAC(+)CPA(+), the hepatic structures were maintained with fewer rejection changes (Fig. 3D). Even on day 14, the TAC(+)CPA(+) protocol protected the CL from severe xenobiotic rejection, with only moderate cellular infiltration in the Glisson capsules (Fig. 3E).

Long-Term Patency of Reconstructed Vessel Circulations

Doppler ultrasonography showed the flow patterns of the arterial inflow and venous outflow in the transplanted CLs on days 14 and 188 in the TAC(+)CPA(−) group. Peak velocities on day 14 were 34.2 (artery) and 9.9 (vein) cm/s, whereas those on day 188 were 12.5 and 3.4 cm/s, respectively (See Figure, Supplemental Digital Content 3, available at http://links.lww.com/SLA/A257).

Long-Term Maintenance of Secretion of Rat Albumin in Nagase Analbuminemia Rats

Although serum rat albumin concentrations in Nagase analbuminemia rat recipients were undetectable before Chimeric liver transplantation, the transplanted CLs produced albumin on day 5 and then maintained production for 4 months, with maintenance of luminescence under the TAC(+)CPA(−) protocol (Fig. 4A).

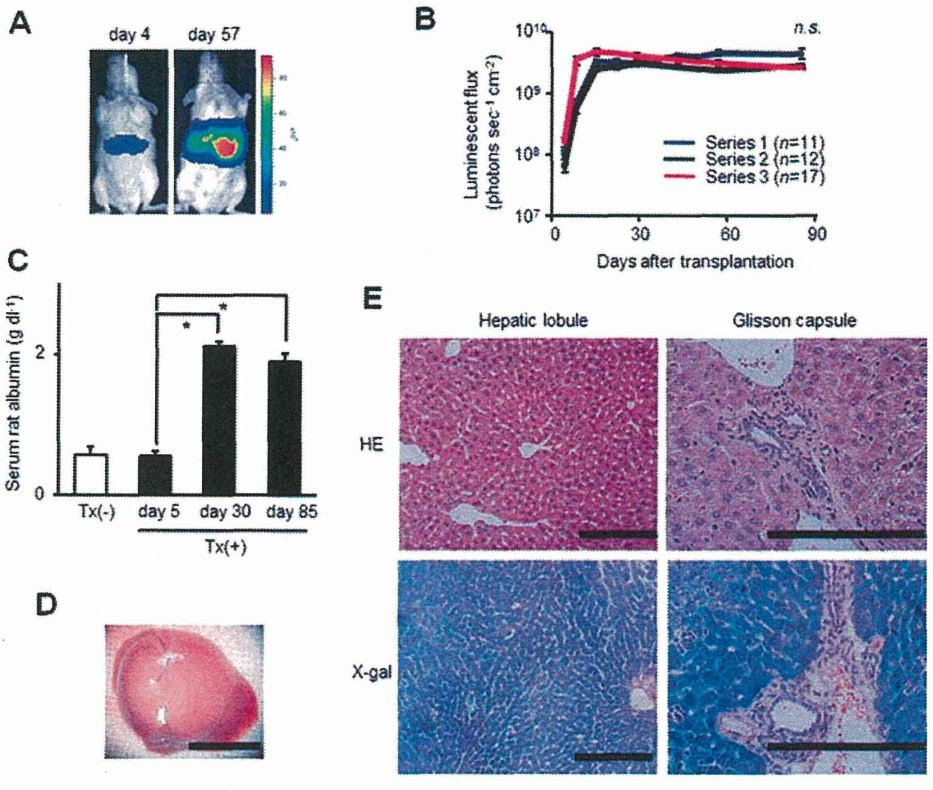

FIGURE 2. Development of CL grafts in uPA/SCID mice. A, Spread of luminescence-positive area. B, Luminescence after hepatocyte transplantation in 3 independent series. *n* as indicated; values are shown as the mean ± SEM; *n.s.*, no significant difference on day 85. C, Production of rat albumin by transplanted rat hepatocytes in mice ($n = 12$). *$P < 0.01$; Values are shown as the mean ± SEM; Tx, hepatocyte transplantation. D, Macroscopic appearance of CL before engraftment. Scale bar = 10 mm. E, hematoxylin-eosin and X-gal staining of intact CLs. The results shown are representative of 5 separate analyses. Scale bars = 200 μm.

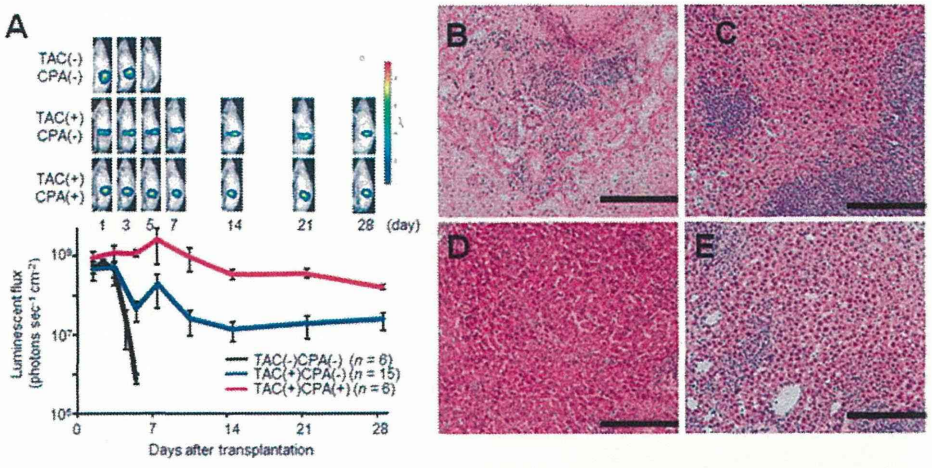

FIGURE 3. Viability of transplanted CL grafts in wild-type LEW rat recipients. A, Luminescence from transplanted CLs. Each in vivo luminescent image is representative of 3 independent groups. *n* as indicated. B–E, Histological analyses of transplanted CLs. The figures present independent recipients. B, Graft with TAC(−)CPA(−) on day 5. C, Graft with TAC(+)CPA(−) on day 7. D, Graft with TAC(+)CPA(+) on day 4. E, Graft with TAC(+)CPA(+) on day 14. Scale bars = 200 μm.

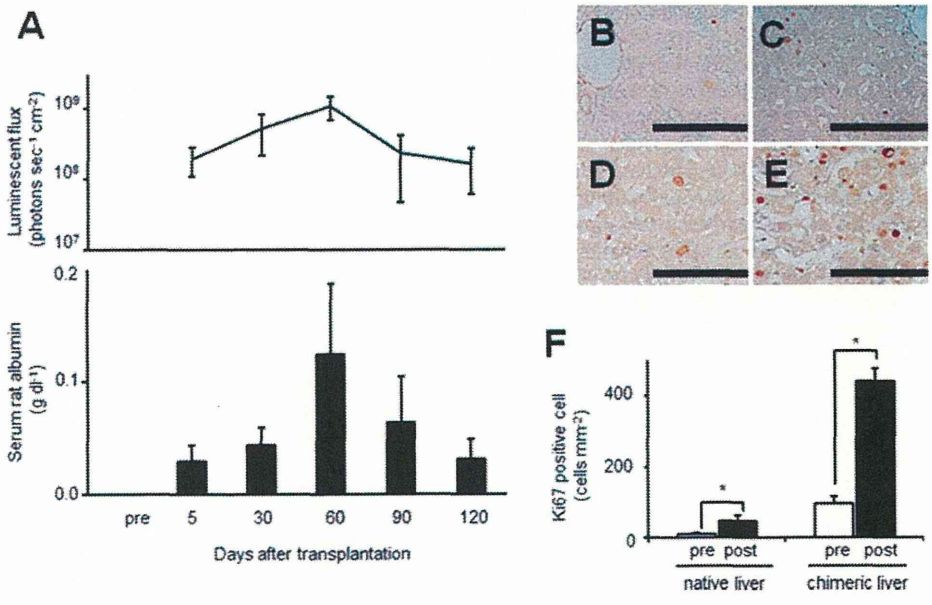

FIGURE 4. A, Luminescence (line) and albumin production (column) from transplanted CLs in Nagase analbuminemia rat recipients ($n = 3$). Values are shown as the mean ± SEM; pre, pre-chimeric liver transplantation. B–F, Immunohistochemical analyses with Ki67. B, C, Recipient native and transplanted CLs, respectively, before host hepatectomy. D, E, Recipient remnant and CLs, respectively, 2 days after recipient left lobectomy. F, Numbers of Ki67-positive cells. Values are shown as the mean ± SEM; pre, prelobectomy; post, postlobectomy.

Self-Regenerative Capacity of Transplanted CL

Ki67 immunohistochemical analyses revealed that Ki67-positive cells were significantly increased in the CLs and in the remnant native livers at 2 days after the left lobectomy in the recipients, as compared with those sampled before the hepatectomy (Fig. 4B–F), suggesting the proliferative potential of the transplanted CLs.

DISCUSSION

The chronic shortage of liver grafts has led to extended criteria for grafts from both deceased[19,20] and living donors,[21] along with ethical issues related to organ trafficking and transplant tourism.[22] Although alternative therapies, such as hepatocyte transplantation,[23] transplantation from non–heart beating donors,[24] bioartificial liver,[25] and xenotransplantation,[26,27] have been intensively investigated to address this situation, none has been found practical because of low stability, low availability, and high antigenicity.

Regenerative approaches have recently been applied to develop engineered organs by focusing on native organs as scaffolds. An approach using a decellularized organ matrix enabled regeneration of syngeneic cells in an animal model,[5,6] though cell repopulation efficiency was still low in ex vivo conditions. Another study injected blastocysts with xenogeneic pluripotent stem cells to produce a chimeric pancreas in a rodent model.[7] However, ubiquitous chimerism in scaffold animals has led to ethical concerns about the formation of chimeric brains and genitalia. Thus, effective and organ-specific engineering is required.

We have developed a strategy to create engineered chimeric "organ" livers with autologous or allogeneic human hepatocytes and other nonparenchymal components from xenogeneic scaffolds in transgenic pigs. This method enables utilization of patent hepatocytes and allogeneic donor cells, and the organogenetic potential in living animals contributes to rapid and timely production of CLs. Moreover, pretreatment with drugs or gene induction in the donor animal may be useful before transplantation.

In this study, we successfully created a rodent model to generate organ-specific engineered CLs, followed by their transplantation. CLs were created in uPA/SCID mice, whose native hepatocytes are injured through accumulation of urokinase-type plasminogen and provide a favorable niche for effective repopulation of transplanted hepatocytes from rats[28] and humans,[11] with a replacement rate greater than 90%.[12] Using hepatocytes derived from transgenic rats with

luciferase or LacZ genes, we found that transplanted hepatocytes in mice spread promptly and stably maintained their viability. Rat albumin production and histological analyses also indicated stable functions and structures of the CLs. These results demonstrated the advantages of CLs with effective productivity and maintenance. Because the CLs were one-eighth smaller than the rat native livers, we transplanted in an auxiliary manner without a hepatectomy or removal of the recipient liver. In addition, we removed the recipient's left kidney to utilize the left renal artery and vein as afferent and efferent vessels, respectively. We considered that a left nephrectomy would not have a large impact on our aim to investigate chimeric liver transplantation feasibility, whereas it might have an influence on recipient's survival. Moreover, though clinical liver transplantation and most rat liver transplantation models reconstruct portal vein circulation, we left it unanastomosed, as we previously reported in a rat auxiliary liver transplantation model,[17] in which the transplanted livers maintained their histological structure.

This analysis revealed severe rejection toward xenogeneic components, resulting in disappearance of luminescence in CLs without immunosuppression. Because humoral rejection was suspected in xenorejection toward the vascular endothelium,[29] we used cyclophosphamide to suppress antibody production in addition to tacrolimus.[18] Our results showed improvement in graft survival in the immunosuppressed groups. TAC(+)CPA(+) showed higher luminescence as compared with TAC(+)CPA(−), though there was no statistical difference between them. On the other hand, histological results showed the superiority of TAC(+)CPA(+). We speculated that these findings indicated antibody-mediated rejection even in Chimeric liver transplantation and that appropriate combination therapies might improve graft survival. Although we previously hypothesized that syngeneic parenchyma might function to protect against rejection toward xenocomponents,[30] the reaction to mouse-origin tissues remained without obvious evidence of attenuation. Further studies to investigate the effects of hepatocytes and specific targets of rejection are required, including those that focus on other aspects such as genetic expressions.[31]

In clinical liver transplantation, thrombotic events can result in graft failure.[32] Ultrasonography showed arterial and venous flow in transplanted CLs even after 6 months, which indicated patency of the anastomosed vessels. We also investigated rat albumin in Nagase analbuminemia rat recipients and demonstrated stable production for a long period. Although the liver possesses a variety of functions and markers,[3,6] albumin analysis showed functions specific to transplanted CLs in Nagase analbuminemia rats with intact livers, which functioned normally except for albumin production. We regarded this result to be preferable in regard to our aim to investigate the feasibility of Chimeric liver transplantation to show those functions in vivo. Interestingly, we found stable luminescence in transplanted CLs of Nagase analbuminemia rat recipients whose hepatocytes were allogeneic to those of other recipients ($RT1^l$ vs $RT1^a$), suggesting the possibility of a hepatocyte bank for use in producing CLs in clinical settings.

Ki67 analyses showed that hepatocytes in the transplanted CLs maintained proliferation potential. Patients with end-stage liver disease are thought to manifest increasing serum hepatotropic growth signals, such as hepatocyte growth factor.[33] It is expected that CLs will have the potential to respond to such signals to maintain and improve viability after transplantation.

Judging from recent technological achievements in transgenic animals, and ethical issues related to primate usage and practical issues of availability and body size, transgenic pigs represent a major candidate for scaffold animals. Although transgenic pigs such as alpha-1,3-galactosyltransferase gene knockout and human decay accelerating factor transgenic pigs show reduced immunological responses toward the host, complete rejection suppression remains difficult and development of appropriate immunosuppressive protocols is important. Moreover, replacement of nonhepatocyte components, especially vascular endothelium, in the CLs of scaffold pigs or development of humanized pigs is expected. However, utilization of xenogeneic porcine scaffolds raise concerns about xenozoonosis such as porcine endogenous retrovirus,[34,35] though the practical possibility of transmission remains uncertain and some reports have shown results without obvious infection.[36] Nevertheless, cautious and longer investigations are indispensable to secure patient safety.

Although further studies that compare conventional liver transplantation models with this model and larger animal models are needed, the realization of this bioengineering strategy with cell sources and transgenic animals might ultimately lead to replacement of human grafts and achievement of liver transplantation without human donors. These results should provide an important contribution toward scaffold-focused engineering of livers and engineered organ transplantation.

CONCLUSIONS

Engineered CLs were successfully transplanted and showed maintenance of function and structure for a long period. Our results suggest that such CLs have potential to be utilized as alternative grafts.

ACKNOWLEDGMENTS

The authors thank J. K. Critser (University of Missouri) for the insightful discussion and S. Enosawa (National Center for Child Health and Development) for the technical expertise regarding hepatocyte isolation. Transgenic rat embryos are available from the National Bio Resource Project for the Rat (nbrprat@anim.med.kyoto-u.ac.jp), and the Rat Resource & Research Center (Dr. Elizabeth Bryda.; RRRC, http://www.rrrc.us/) in USA.

REFERENCES

1. Thuluvath PJ, Guidinger MK, Fung JJ, et al. Liver transplantation in the United States, 1999–2008. *Am J Transplant.* 2010;10:1003–1019.
2. Yeh H, Smoot E, Schoenfeld DA, et al. Geographic inequity in access to livers for transplantation. *Transplantation.* 2011;91:479–486.
3. Ohashi K, Yokoyama T, Yamato M, et al. Engineering functional two- and three-dimensional liver systems in vivo using hepatic tissue sheets. *Nat Med.* 2007;13;880–885.
4. Soto-Gutiérrez A, Kobayashi N, Rivas-Carrillo JD, et al. Reversal of mouse hepatic failure using an implanted liver-assist device containing ES cell-derived hepatocytes. *Nat Biotechnol.* 2006;24:1412–1419.
5. Ott HC, Matthiesen TS, Goh SK, et al. Perfusion-decellularized matrix: using nature's platform to engineer a bioartificial heart. *Nat Med.* 2008;14:213–221.
6. Uygaun BE, Soto-Gutierrez A, Yagi H, et al. Organ reengineering through development of a transplantable recellularized liver graft using decellularized liver matrix. *Nat Med.* 2010;16:814–820.
7. Kobayashi T, Yamaguchi T, Hamanaka S, et al. Generation of rat pancreas in mouse by interspecific blastocyst injection of pluripotent stem cells. *Cell.* 2010;142:787–799.
8. Ekser B, Rigotti P, Gridelli B, et al. Xenotransplantation of solid organs in the pig-to-primate model. *Transpl Immunol.* 2009;21:87–92.
9. Klymiuk N, Aigner B, Brem G, et al. Genetic modification of pigs as organ donors for xenotransplantation. *Mol Reprod Dev.* 2010;77:209–221.
10. Locke JE, Sun Z, Warren DS, et al. Generation of humanized animal livers using embryoid body-derived stem cell transplant. *Ann Surg.* 2008;248;487–493.
11. Mercer DF, Schiller DE, Elliott JF, et al. Hepatitis C virus replication in mice with chimeric human livers. *Nat Med.* 2001;7:927–933.
12. Tateno C, Yoshizane Y, Saito N, et al. Near completely humanized liver in mice shows human-type metabolic responses to drugs. *Am J Pathol.* 2004;165:901–912.

13. Hakamata Y, Murakami T, Kobayashi E. "Firefly rats" as an organ/cellular source for long-term in vivo bioluminescent imaging. *Transplantation*. 2006;81:1179–1184.
14. Horie M, Sekiya I, Muneta T, et al. Intra-articular injected synovial stem cells differentiate into meniscal cells directly and promote meniscal regeneration without mobilization to distant organs in rat massive meniscal defect. *Stem Cells*. 2009;27:878–887.
15. Oren R, Dabeva MD, Petkov PM, et al. Restoration of serum albumin levels in Nagase analbuminemic rats by hepatocyte transplantation. *Hepatology*. 1999;29:75–81.
16. Enosawa S, Suzuki S, Li XK, et al. Higher efficiency of retrovirus transduction in the late stage of primary culture of hepatocytes from nontreated than from partially hepatectomized rat. *Cell Transplant*. 1998;7:413–416.
17. Rong Xiu D, Hishikawa S, Sato M, et al. Rat auxiliary liver transplantation without portal vein reconstruction: comparison with the portal vein-arterialized model. *Microsurgery*. 2001;21:189–195.
18. Murase N, Starzl TE, Demetris AJ, et al. Hamster-to-rat heart and liver xenotransplantation with FK506 plus antiproliferative drugs. *Transplantation*. 1993;55:701–708.
19. Durand F, Renz JF, Alkofer B, et al. Report of the Paris consensus meeting on expanded criteria donors in liver transplantation. *Liver Transpl*. 2008;14:1694–1707.
20. Renz JF, Kin C, Kinkhabwala M, et al. Utilization of extended donor criteria liver allografts maximizes donor use and patient access to liver transplantation. *Ann Surg*. 2005;242:556–565.
21. Trotter JF, Adam R, Lo CM, et al. Documented deaths of hepatic lobe donors for living donor liver transplantation. *Liver Transpl*. 2006;12:1485–1488.
22. Steering Committee of the Istanbul Summit. Organ trafficking and transplant tourism and commercialism: the Declaration of Istanbul. *Lancet*. 2008;372:5–6.
23. Dhawan A, Puppi J, Hughes RD, et al. Human hepatocyte transplantation: current experience and future challenges. *Nat Rev Gastroenterol Hepatol*. 2010;7:288–298.
24. Selck FW, Grossman EB, Ratner LE, et al. Utilization, outcomes, and retransplantation of liver allografts from donation after cardiac death: implications for further expansion of the deceased-donor pool. *Ann Surg*. 2008;248:599–607.
25. Demetriou AA, Brown RS, Busuttil RW, et al. Prospective, randomized, multicenter, controlled trial of a bioartificial liver in treating acute liver failure. *Ann Surg*. 2004;239:660–670.
26. Starzl TE, Fung J, Tzakis A, et al. Baboon-to-human liver transplantation. *Lancet*. 1993;341:65–71.
27. Ekser B, Gridelli B, Tector AJ, et al. Pig liver xenotransplantation as a bridge to allotransplantation: which patients might benefit? *Transplantation*. 2009;88:1041–1049.
28. Giannini C, Morosan S, Tralhao JG, et al. A highly efficient, stable, and rapid approach for ex vivo human liver gene therapy via a FLAP lentiviral vector. *Hepatology*. 2003;38:114–122.
29. Ghebremariam YT, Smith SA, Anderson JB, et al. Intervention strategies and agents mediating the prevention of xenorejection. *Ann N Y Acad Sci*. 2005;1056:123–143.
30. Goto S, Lord R, Kobayashi E, et al. Novel immunosuppressive proteins purified from the serum of liver-retransplanted rats. *Transplantation*. 1996;61:1147–1151.
31. Tahara K, Murakami T, Fujishiro J, et al. Regeneration of the rat neonatal intestine in transplantation. *Ann Surg*. 2005;242:124–132
32. Bekker J, Ploem S, de Jong KP. Early hepatic artery thrombosis after liver transplantation: a systematic review of the incidence, outcome and risk factors. *Am J Transplant*. 2009;9:746–757.
33. Tomiya T, Omata M, Imamura H, et al. Impaired liver regeneration in acute liver failure: the significance of cross-communication of growth associated factors in liver regeneration. *Hepatol Res*. 2008;38:S29–S33.
34. Mueller NJ, Takeuchi Y, Mattiuzzo G, at al. Microbial safety in xenotransplantation. *Curr Opin Organ Transplant*. 2011;16:201–206.
35. Onions D, Cooper DK, Alexander TJ, et al. An approach to the control of disease transmission in pig-to-human xenotransplantation. *Xenotransplantation*. 2000;7:143–155.
36. Michaels MG, Kaufman C, Volberding PA, et al. Baboon bone-marrow xenotransplant in a patient with advanced HIV disease: case report and 8-year follow-up. *Transplantation*. 2004;78:1582–1589.

Dig Dis Sci
DOI 10.1007/s10620-012-2514-8

ORIGINAL ARTICLE

Cytoglobin May Be Involved in the Healing Process of Gastric Mucosal Injuries in the Late Phase Without Angiogenesis

Fumio Tanaka · Kazunari Tominaga · Eiji Sasaki · Mitsue Sogawa · Hirokazu Yamagami · Tetsuya Tanigawa · Masatsugu Shiba · Kenji Watanabe · Toshio Watanabe · Yasuhiro Fujiwara · Norifumi Kawada · Katsutoshi Yoshizato · Tetsuo Arakawa

Received: 30 July 2012 / Accepted: 3 December 2012

Abstract
Background and Aims Cytoglobin (Cygb) is the newest globin family and is upregulated during hypoxia to maintain the oxygen status. Herein, we investigated Cygb expression in both acute and chronic gastric mucosal injuries.
Methods Acute gastric mucosal injuries in rats were produced by oral administration of indomethacin, followed by sacrifice at 1, 3, 6, 24, and 48 h. Gastric ulcer was produced by acetic acid, followed by sacrifice on days 3, 7, 11, 18, and 25. Each protein expression of Cygb and hypoxia-inducible factor (HIF)-1α was evaluated by western blotting. We measured vascular endothelial growth factor (VEGF) mRNA by RT-PCR and examined localization of Cygb by immunofluorescence.
Results In indomethacin-induced injury, Cygb protein was significantly increased at 24 h. In ulcerated tissues, HIF-1α protein was significantly increased on days 7 and 11 (1.83 ± 0.11 and 2.12 ± 0.19 folds, respectively, $p < 0.05$ and 0.01), which corresponded to the early healing phase. In contrast, Cygb protein was significantly increased on days 11 and 18 (1.87 ± 0.13 and 1.60 ± 0.06 folds, respectively, $p < 0.05$), which demonstrated late phase. Though these proteins peaked on day 11, VEGF mRNA was gradually increased from day 11 to 18. Cygb was expressed in fibroblasts and myofibroblasts in both acute and chronic models. Cygb and HIF-1α were abundantly colocalized at the ulcer margin before angiogenesis development. However, faint localization was observed with angiogenesis.
Conclusions Cygb may be involved in the healing process of gastric mucosal injuries in the late phase without angiogenesis.

Keywords Stomach ulcer · Hypoxia · Angiogenesis · Mesenchyme · Fibroblast

Abbreviations

Cygb	Cytoglobin
NO	Nitric oxide
HRE	Hypoxia response element
HIF	Hypoxia-inducible factor
VEGF	Vascular endothelial growth factor
RT-PCR	Reverse transcription-polymerase chain reaction
α-SMA	α-smooth muscle actin
vWF	von Willebrand factor

Introduction

Cytoglobin (Cygb), a globin similar to myoglobin, was discovered by the proteomics approach of rat hepatic stellate cells in 2001 [1]. The expression of Cygb was

F. Tanaka · K. Tominaga (✉) · M. Sogawa · H. Yamagami · T. Tanigawa · M. Shiba · K. Watanabe · T. Watanabe · Y. Fujiwara · T. Arakawa
Department of Gastroenterology, Graduate School of Medicine, Osaka City University, 1-4-3 Asahimachi, Abeno-ku, Osaka 545-8585, Japan
e-mail: tomy@med.osaka-cu.ac.jp

E. Sasaki
Department of Gastroenterology, Osaka City General Hospital, Osaka, Japan

N. Kawada
Department of Hepatology, Graduate School of Medicine, Osaka City University, Osaka, Japan

K. Yoshizato
PhoenixBio Co, Ltd, Hiroshima, Japan

Published online: 10 January 2013

detected in normal rat and human tissues such as brain, heart, kidney, lung, liver, stomach, intestine, trachea, and liver [2]. Immunohistochemistry and immunoelectron microscopy revealed that Cygb was localized in fibroblast-like cells in splanchnic organs, namely, the vitamin A-storing cell lineage; however, Cygb was not localized in epithelial cells, endothelial cells, muscle cells, blood cells, macrophages, or dermal fibroblasts [3]. Cygb plays a potential protective role against hypoxia. It functions as a scavenger of nitric oxide (NO) or reactive oxygen species and as an oxygen transporter and sensor [4–6]. Cygb functions as an intracellular oxygen transporter because this protein has 40 % amino acid sequence homology with myoglobin [7]. Cygb may act as a protein supplying oxygen to O_2-requiring cellular reactions unrelated to mitochondrial respiration [6]. In addition, it exhibits dioxygenase enzymatic activity and plays a role in fibrotic organ disorder [3, 8].

Cygb expression is upregulated under hypoxic conditions in vitro and in vivo [9, 10]. Upregulation of Cygb mRNA upon exposure to a hypoxic condition is observed in mouse and rat brain, skeletal muscle, liver, and heart. Analysis of the human Cygb promoter region revealed the presence of hypoxia response element (HRE) in the 5′ UTR region of the *CYGB* gene, which suggested that it might have an oxygen-dependent regulation. Several lines of evidence suggested that Cygb was hypoxia-inducible [4, 10]. A previous study showed that the binding of hypoxia-inducible factor-1 (HIF-1) protein to HRE motifs directly induced the promotion of Cygb transcription under hypoxic conditions in vitro [11].

Ischemia and tissue hypoxia induce vasodilatation and angiogenesis to maintain blood flow. Many vasoactive substances and angiogenic factors, such as vascular endothelial growth factor (VEGF), are expressed in response to hypoxia to induce angiogenesis. VEGF, an endothelial cell-specific mitogen, is the most potent angiogenic growth factor [12]. VEGF has been implicated in the angiogenic response to gastric ulceration and ethanol-induced gastric erosions [13, 14]. Hypoxia induces VEGF expression via HIF-1 which is a transcription factor composed of two subunits: HIF-1α and HIF-1β [15, 16]. Under normoxic conditions, the HIF-1β protein is relatively stable, whereas the HIF-1α protein is continuously produced and rapidly degraded. In contrast, hypoxia stabilizes the HIF-1α protein leading to its accumulation within the cell and formation of active HIF-1 complex [17]. HIF-1α is the key factor that induces angiogenesis during the healing of gastric ulcer, nonsteroidal anti-inflammatory drug-induced gastric mucosal lesion, and esophageal ulcer [18, 19]. In addition, HIF-1 is recognized as the master regulator of the cellular hypoxia responses [20]. A recent study demonstrated that the expression of Cygb was altered in HIF knockout mice, supporting an important role for HIF in Cygb expression [4, 11].

Healing of gastric ulcers involves many vasoactive substances and angiogenic factors, including endothelin, NO, and VEGF [13]. These factors are known to be induced by HIF-1α that was highly expressed during the early phase of gastric ulcer healing [15]. However, the pathophysiological role of Cygb in mucosal injury of the stomach has remained to be elucidated. The aim of this study was to investigate Cygb expression and its possible involvement in the repair process of gastric mucosal injuries in rat.

Materials and Methods

Animals

All experimental procedures were approved by the Animal Care Committee of Osaka City University Graduate School of Medicine. In this study, we used 8-week-old male Wistar rats (purchased from Clea Japan, Osaka, Japan) weighing about 200 g. The animals were given standard rat chow diet (CE-2; Clea Japan) and water ad libitum.

Production of Acute Gastric Mucosal Injury

Rats were starved for 24 h before the experiment as follows; acute gastric injury was induced by oral administration of indomethacin or HCl-EtOH according to the method described in a previous report ($N = 3$) [21, 22]. Indomethacin was suspended in 0.5 % methyl cellulose and administered at a dose of 20 mg/kg. Rats were administered 0.15 N HCl in 60 % EtOH (0.5 mL/100 g).

Production of Experimental Gastric Ulcer

Experimental gastric ulcers were produced in rats according to the method described in a previous report [23, 24]. In brief, rats were fasted for 12 h and laparotomy was performed under ether anesthesia. A round plastic mold (6 mm in diameter) was placed tightly on the anterior serosal surface of the antral-oxyntic border. Acetic acid (100 %, 0.06 mL) was poured into the mold and allowed to remain on the gastric wall for 60 s ($N = 5$–6). In control rats, laparotomy was performed under ether anesthesia and their abdomens were closed without the above treatment (sham-operated rats, $N = 5$–6).

Experimental Protocol

In acute gastric injury models, rats were killed by cervical dislocation at the following time after drug administration:

1, 3, 6, 24, and 48 h in the indomethacin model, and 0.5, 2, 6, and 24 h in the HCl-EtOH model. For histological study, rats were killed at 48 h in the indomethacin model. Stomachs were rapidly excised and opened along the greater curvature. Tissues were rinsed in saline and the extent of gastric damage was evaluated by calculating the total length of the macroscopically visible erosions. Gastric tissues were cut to a size of 5 × 5 mm for western blotting and 5 × 10 mm for immunofluorescence. These tissues were frozen in liquid nitrogen and stored at −80 °C until the assay.

In the experimental gastric ulcer model, rats were killed on days 3, 7, 11, 18, or 25 after gastric ulcer formation, and the ulcerated gastric tissues (total gastric walls including ulcerated area, weighing 100–120 mg) were rapidly removed. As control tissues, intact gastric tissues (in the same region as ulcerated tissues) were rapidly excised from sham-operated rats. These tissues were rinsed in saline, frozen in liquid nitrogen, and stored at −80 °C until protein assay was performed. For quantitative real-time reverse transcription-polymerase chain reaction (RT-PCR), rats were killed on days 11 and 18, and their stomachs were removed and processed as described below. For histological study, the rats were killed on day 11.

Western Blot Analysis

Expression of Cygb and HIF-1α proteins were examined by western blotting. Gastric tissues were homogenized and lysed on ice in buffer containing 0.5 % Nonident P-40, 40 mM Tris–HCl (pH 8.0), 120 mM NaCl, 1 mM phenylmethylsulfonyl fluoride (PMSF), and 10 μg of leupeptin per milliliter. The protein content of the lysate was measured with a modified bicinchoninic acid method (BCA) protein assay reagent kit (Pierce, IL, USA). Proteins were denatured with sodium dodecyl sulfate (SDS) sample buffer and subjected to 10 % SDS–polyacrylamide gel electrophoresis (PAGE) and transferred to a polyvinylidene difluoride membrane. Membranes were blocked in TBS buffer [10 mM Tris–HCl (pH 7.5), 100 mM NaCl, 0.1 % Tween-20] containing 5 % bovine serum albumin (BSA), and then incubated with the specific polyclonal antibody against Cygb (diluted 1:1,000) or monoclonal antibody against HIF-1α (1:500) overnight. The bound antigen–antibody complexes were detected with anti-rabbit IgG-horseradish peroxidase (HRP) by using enhanced chemiluminescence in accordance with the manufacturer's instructions (Amersham, IL, USA). Relative expressions were represented as percentages of sham-operated rats (controls).

Quantitative Real-Time RT-PCR

We measured mRNA expression of HIF-1α and VEGF in the ulcerated gastric tissues by quantitative real-time RT-PCR. Real-time RT-PCR analyses were performed by using the previously described protocol [25]. Glyceraldehyde-3-phosphate dehydrogenase (GAPDH) was used as an internal standard with Taqman GAPDH control reagents (PE Applied Biosystems). The mean value in the sham-operated tissues (controls) was taken as 1.

Antibodies

Rabbit polyclonal IgG antibodies against rat Cygb were produced by using a synthetic NH_2-terminal polypeptide of rat Cygb, namely, NH_2-MEKVPGDMEIERRERNEE + Cys-COOH, as an immunogen as described previously [1]. Other antibodies used for immunohistochemistry were as follows: vimentin was detected with mouse monoclonal antibody (Abcam, Tokyo, Japan), α-smooth muscle actin (α-SMA) with mouse monoclonal antibody (Sigma-Aldrich, MO, USA), cytokeratin with mouse monoclonal antibody (Abcam), HIF-1α with mouse monoclonal antibody (Santa Cruz Biotechnology, CA, USA), and von Willebrand factor (vWF) with mouse monoclonal antibody (Santa Cruz). Cygb immunoreactivity was detected using an Alexa Fluor 488-conjugated secondary antibody (Alexa Fluor 488 donkey anti-rabbit, Molecular Probes Inc., OR, USA). Others were detected using an Alexa Fluor 594-conjugated secondary antibody (Alexa Fluor 594 donkey anti-mouse, Molecular Probes). Nuclei were counterstained with DAPI (ProLong Gold antifade reagents with DAPI, Molecular Probes).

Indirect Immunofluorescence

Excised and cut stomachs were embedded in Tissue-Tek® OCT compound (Sakura Finetechnical Co., Ltd., Tokyo, Japan) and then frozen in dry ice. Tissues were cut to 6-μm cryostat sections and mounted on silane-coated glass slides and air dried. And then, the samples were fixed with acetone for 7 min. The sections were incubated with 5 % donkey serum in phosphate-buffered saline (PBS) for 60 min to reduce nonspecific antibody binding and incubated with the specific first antibodies overnight at 4 °C. All antibodies were diluted to 1:250 in Dako antibody diluent with background reducing components (Dako, Tokyo, Japan). After washing with PBS, the sections were incubated with secondary antibodies for 60 min at room temperature. After washing with PBS, sections were mounted using ProLong Gold antifade reagents with DAPI. Tissues were examined with a fluorescent microscope (Olympus BX50, Tokyo, Japan).

Statistical Analysis

Significant differences were assessed by one-way analysis of variance (ANOVA) with Tukey–Kramer post hoc test.

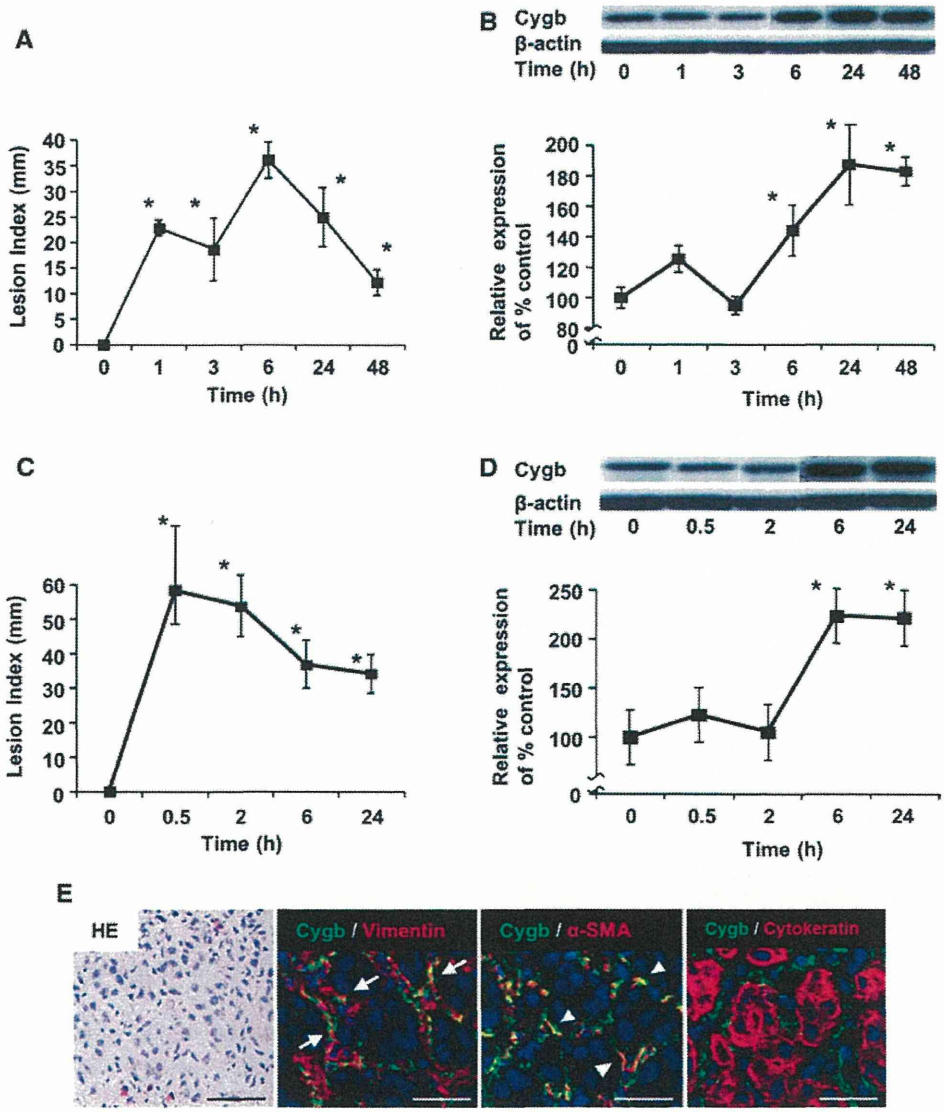

Fig. 1 Cygb protein expression in acute gastric injury models. Lesion index (**a**) and expression of Cygb protein (**b**) in indomethacin-induced gastric mucosal injury. Lesion index (**c**) and expression of Cygb protein (**d**) in HCl-EtOH-induced gastric mucosal injury. Each value represents the mean ± SEM ($N = 3$). *$p < 0.05$ versus control. **e** Localization of Cygb at 48 h after the production of indomethacin-induced acute gastric mucosal injury. The mucosal layer was slightly edematous and the structure of gland was distorted (*first panel* from *left*). Colocalization was observed in the spindle-shaped or linear-shaped cells surrounding the glands, which were indicated to be fibroblasts or myofibroblasts (*second panel, arrow*). Colocalization of Cygb and α-SMA was also observed in the linear-shaped cells, which confirmed the cells were myofibroblasts (*third panel, arrowheads*). Cygb was not expressed in the epithelial cells which were immunoreactive for cytokeratin (*fourth panel*). *HE* hematoxylin and eosin. *Scale bars* 50 μm

Values are expressed as mean ± standard error of mean (SEM). Probability values of less than 0.05 were considered to indicate statistical significance.

Results

Expression of Cygb in Acute Gastric Mucosal Injury Model

In an indomethacin-induced acute injury model, expression of the Cygb protein was increased at 6 h when the lesion index was maximum, and it peaked at 24 h (1.87 ± 0.26 fold, $p < 0.05$ vs. control group; Fig. 1a, b). In the HCl-EtOH model, maximal expression of Cygb protein was observed from 6 to 24 h, while mucosal injury peaked at 0.5 h after HCl-EtOH administration (Fig. 1c, d). These results showed that the level of Cygb protein was increased in the late phase of mucosal healing.

Localization of Cygb in Acute Gastric Mucosal Injury Model

At 48 h after the production of indomethacin-induced acute gastric mucosal injury, Cygb protein expression was still high (Fig. 1b). At the same time, gastric mucosa was quite recovered from erosion and the lesion index was low (Fig. 1a). The mucosal layer was slightly edematous and the structure of gland was distorted (Fig. 1e, first panel from left). Cygb and vimentin were colocalized in the cytoplasm of mesenchymal cells surrounding the glands (second panel). Colocalization was observed in the